A

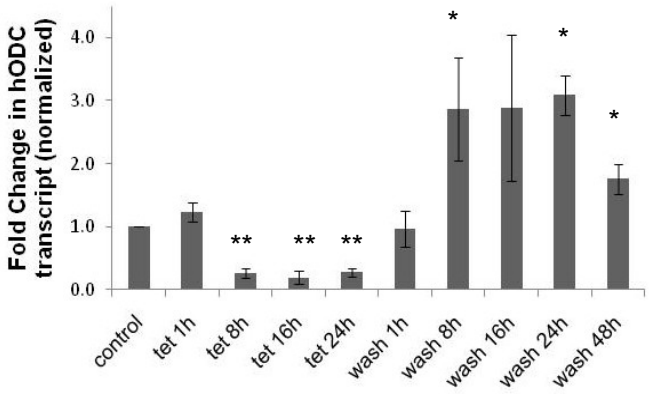

B

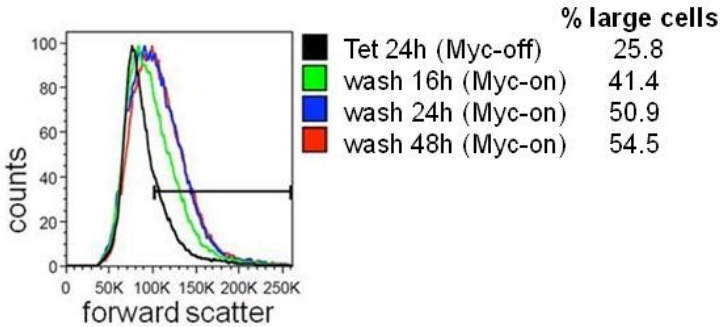

C

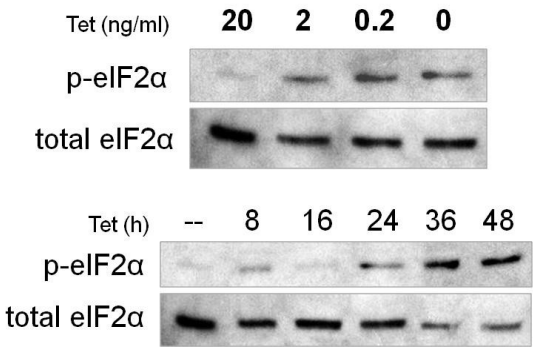

Supplementary Figure 1

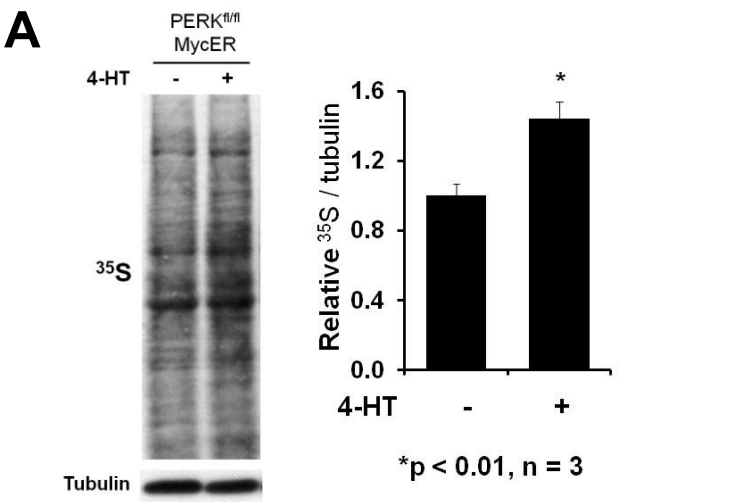

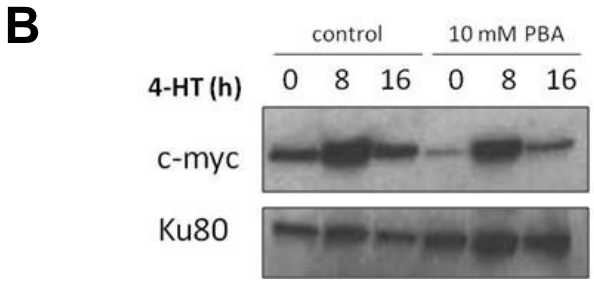

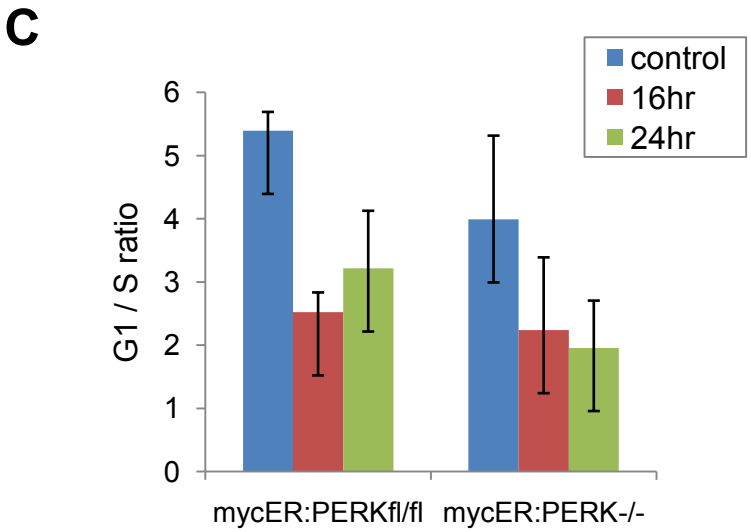

Supplementary Figure 2

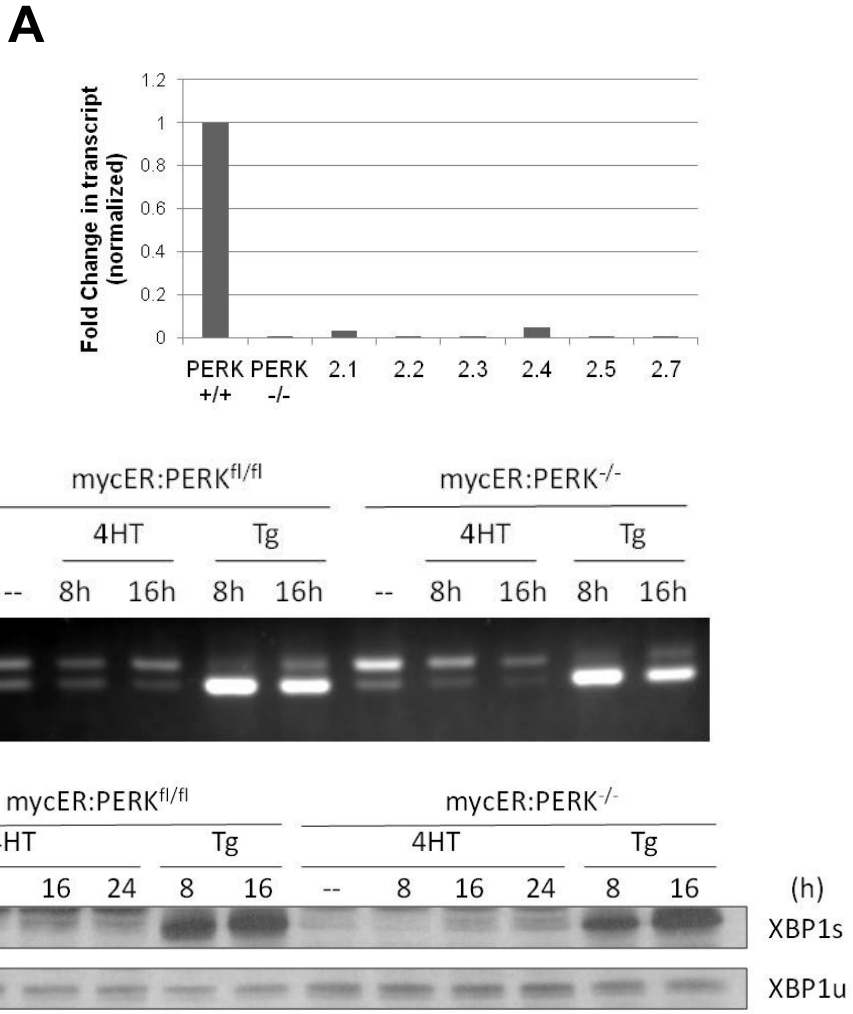

Supplementary Figure 3

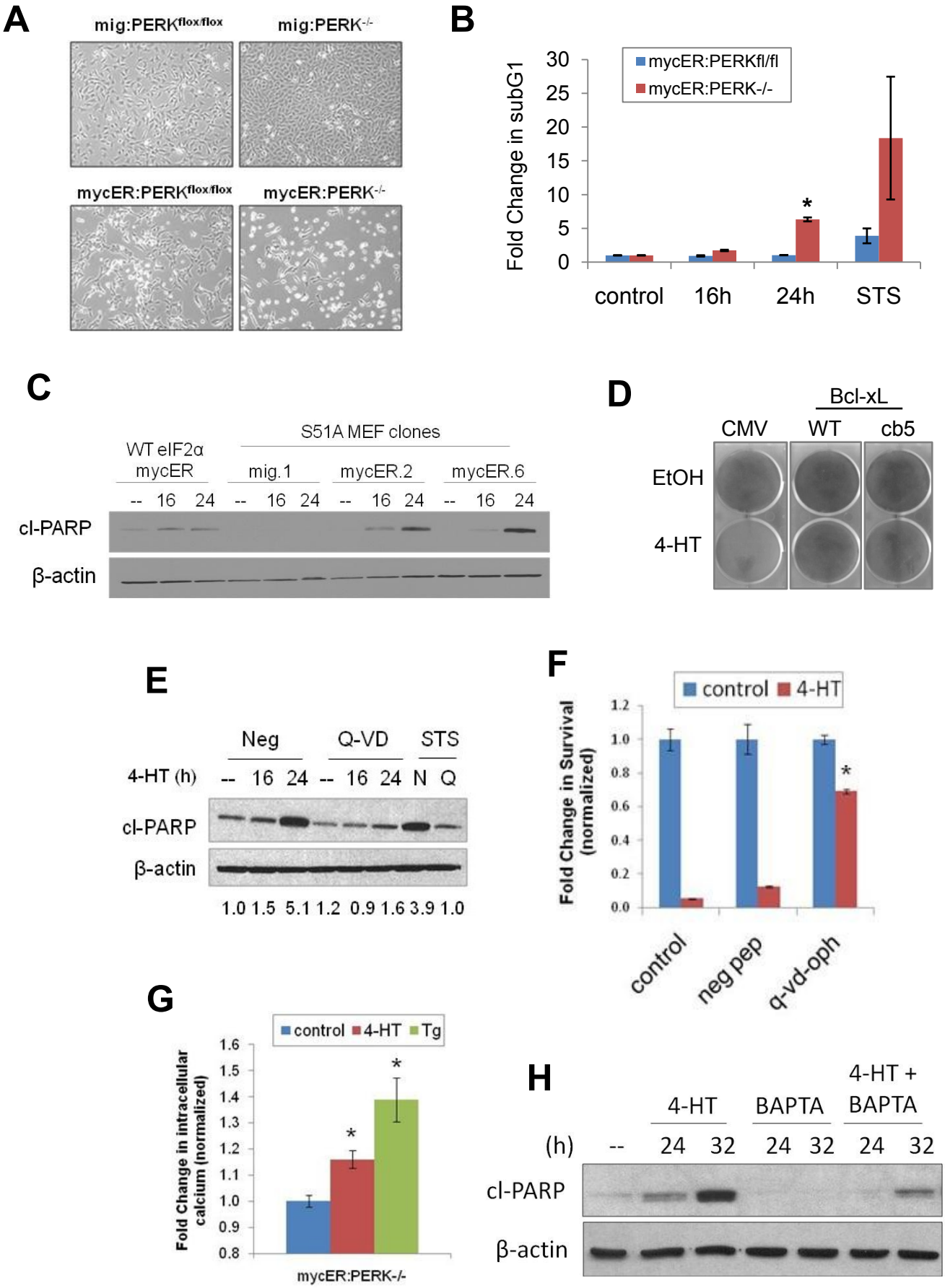

Supplementary Figure 4

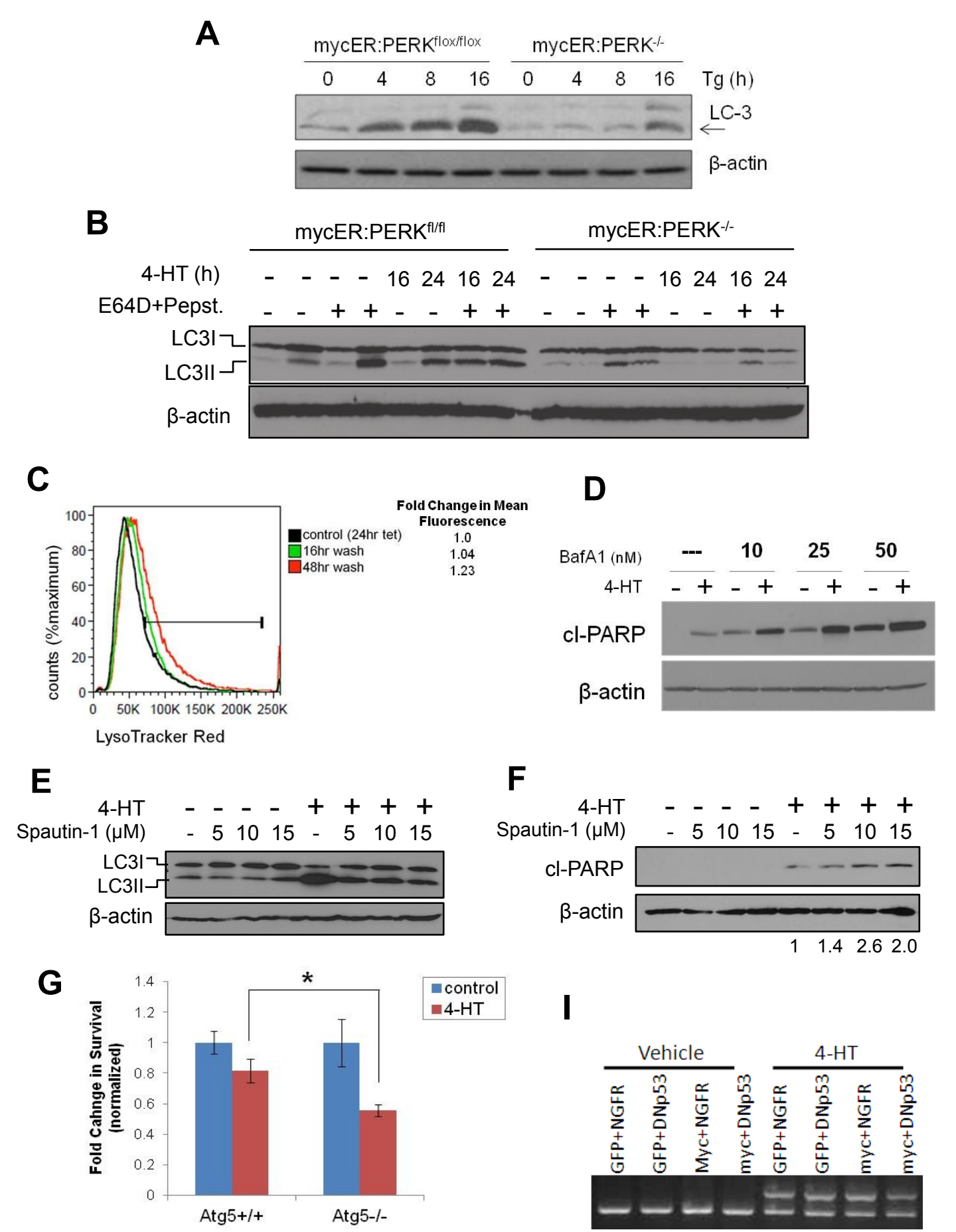

Supplementary Figure 5

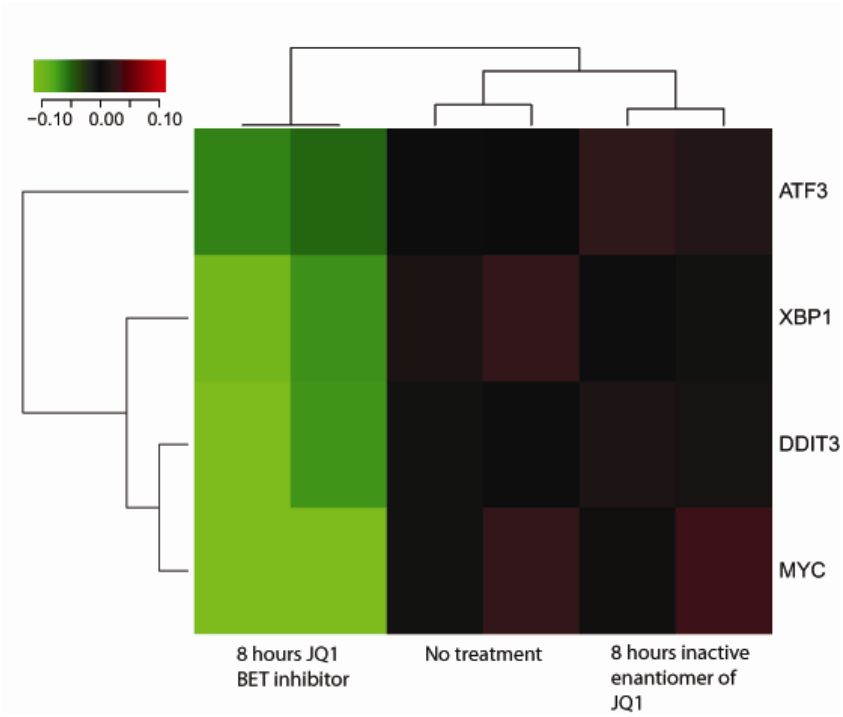

Supplementary Figure 6

SUPPLEMENTARY INFORMATION

Supplementary Methods

RT-PCR and Real Time Quantitative PCR

RT-PCR and DNA gel electrophoresis were performed to measure XBP1 splicing. The primers amplify both total and spliced XBP1, which differ in size by 26bp and are resolved on a 2.5% agarose gel. The following primers were used: mXBP1-F: 5'-AAGTGGTGGATTTGGAAGAAGA and mXBP1-R: 5'-TCTGCTAGTCTGGAGGAACTCC. Real Time PCR analysis was performed with Power SYBR Green PCR Master Mix (Applied Biosystems) on a 7300 Real Time PCR System (Applied Biosystems) using the Standard Curve method. The following primers were used for Real Time PCR assays: human XBP1s-F: 5'-CCGCAGCAGGTGCAGG, and XBP1s-R: 5'-GAGTCAATACCGCCAGAATCCA; human ODC-F: 5'-TTGCGGATTGCCACTGATGATTCC, and ODC-R: 5'-ATCAGAGATTGCCTGCACGAAGGT; human 18S-left: 5'-CAATTACAGGGCCTCGAAAG, and 18S-right: 5'-AAACGGCTACCACATCCAAG; human ATF3-left: 5'-TAGGCTGGAAGAGCCAAAGA, and ATF3-right: 5'-TTCTCACAGCTGCAAACACC; and mouse PERK-left: 5'-CAAGCTATACATGAGCCCAGAG, and PERK-right: 5'- GTGCTGAATGGGTAGAGGAGTT.

Immunobloting (Antibodies)

The following antibodies were used in overnight incubations at 4°C: c-Myc (Santa Cruz sc-764, and Sigma M4439), p-eIF2α (Cell Signaling, #9721), total eIF2α (Cell Signaling, #9722), ATF4 (Santa Cruz, sc-200), XBP1 (Santa Cruz, sc-7160), p-PERK (Cell Signaling, #3179; Biolegend, #649401), total PERK (Cell Signaling, sc-13073), N-Myc (Santa Cruz, sc-53993), PARP (Cell Signaling, #9532), mouse specific cleaved-PARP (Cell Signaling, #9544), LC-3 (Cell Signaling, #2775), p62 (Sigma, P0067), ULK1 (Sigma, P0068), Ku80 (human Calbiochem, NA-52; mouse Cell Signaling, #2753), and β-actin (Sigma). Membranes were incubated with HRP-conjugated secondary anti-mouse or anti-rabbit antibodies (Thermo Scientific, #31430, #31460) for 2 hours at room temperature and HRP detection was performed with ECL-Plus Chemiluminescence (GE Life Sciences).

Luciferase Assays

MEFs expressing the 5'-UTR-ATF4-luciferase construct were plated in 24-well plates, treated with 4-HT or thapsigargin, and luciferase expression was measured according to the manufacturer's protocols (Dual-Luciferase® Reporter Assay System, Promega). Results were normalized to CMV-Renilla luciferase and are shown as fold change over control.

Calcium Measurements

$[Ca^{2+}]_i$ was measured by dual wave length fluorescence microscopy using a Zeiss AxioVision system as described previously (1). Briefly, cells were cultured on cover slips and then incubated with Fura-2AM for 20 min, then perfused with Krebs-Ringer bicarbonate buffer with 10 mM glucose and 0.25% BSA at a flow rate of 1 mL/min for 5 min. $[Ca^{2+}]_i$ was measured from 10 to 15 individual cells and values are expressed as average of $[Ca^{2+}]_i$ measured in 5 min normalized to control cells.

Gene expression Meta-Analysis

For the meta-analysis, we used information from Mertz *et al*., 2011 (2). In their study, Raji (Burkitt's lymphoma) cells, were treated for eight hours with a BET bromodomain inhibitor, JQ1, and expression array data generated for biological duplicates (no treatment-GSM728964 and GSM728968; JQ1 treatment for eight hours – GSM7288966 and GSM7298980; inactive enantiomer for eight hours – GSM7288978 and GSM72889883) using an Affymetrix GeneChip Human Exon 1.0 ST chips (2). Data from this experiment was downloaded as raw data from ArrayExpress (http://www.ebi.ac.uk/arrayexpress/; E-GEOD-29449). Array data was uploaded into geWorkbench (3) together with a csv-formatted transcript annotation file Exon 1.0ST chips downloaded from Affymetrix and grouped according to treatment condition. The array data were normalized with a microarray-based centering method embedded within geWorkbench. A UPR-associated gene signature consisting of DDIT3 (CHOP), c-MYC, XBP1and ATF3 was uploaded and the data subjected to hierarchical clustering with this signature, applying a Pearson Correlation coefficient with a total linkage setting. The resulting heatmap represents high (red) and low (green) gene expression for each individual sample. The data has been log transformed and median centered.

In order to explore the association between c-Myc status and the expression of ER stress and unfolded protein response signatures we performed an analysis of a clinical dataset for which c-Myc status was established both by fluorescence in situ hybridisation and by expression array profiling. We downloaded the raw data as .CEL files from the NCBI GEO database (accession number: GSE4475). Clinical annotation was downloaded from the same link. The .CEL files were uploaded into Agilent Genespring software (version 12) and normalisation and quality control undertaken. Two signatures were then used. A signature was generated from a paper by Harding *et al*. (4), in which they defined genes that were responsive to ER stress treatment including tunicamycin and for which these responses diminished by knocking out ATF4 and PERK. This signature was developed from Figure 2 and Table 1 of this paper. Since this work used knockout mouse embryonic fibroblasts and the Hummel dataset used human samples we established genelist consisting of human homologues of the genes reported in the Harding paper. We like to thank Harding and the Ron Lab for providing Figure 2

in table format which facilitated the search for human homologues. We then used these two gene signatures to run a gene-level interpretation of the Hummel data and generate data tables containing the Log fold signals for the genes in these lists across all samples. This data was then used in a Pearson complete correlation analysis for hierarchical clustering. The threshold for significance at each of the branchpoints in the hierarchical clusters was set at a p value of <0.05. Pseudo-coloured heatmaps were generated in which the signals for gene expression are depicted on a scale from -1 to +1, achieving a median signal of 0 for each signature independently based on the all of the genes and samples in each analysis. +1 is depicted in red representing maximal expression and -1 is depicted in green representing minimal expression. No differential expression (0) is depicted in black. We then used the clinical annotation available for the samples to annotate the resultant heatmap. The Ig-Myc annotation is derived from the clinical annotation file uploaded onto GSE4475. This reflects the fact that interphase fluorescence in situ hybridization was performed on frozen or paraffin-embedded tissues from 217 cases with the use of probes for *IGH, IGK, IGL, myc, BCL6* and *BCL2* loci. Tumor-biopsy specimens in which *myc* was fused to *IGH, IGK,* or *IGL* were referred to as "*IG-myc*" lymphomas in the paper. IG-Myc status closely correlates with increased c-Myc expression in the array data.

^{35}S Labeling

Cells (250,000 per well) were seeded onto 6 well dishes. 4-hydroxytamoxifen (250nM, Sigma) or vehicle (ethanol) was added to cultures growing in DMEM supplemented with 10% FBS and Pen/Strep for 24 hours to activate Myc. Culture media was changed to DMEM lacking Methionine and Cysteine (CellGro) for 1 hour. 33µCi of radiolabeled Methionine and Cysteine (Express protein labeling mix, Perkin Elmer) per well was added to the culture media for an additional 1 hour of incubation. Cells were harvested and protein was extracted in RIPA lysis buffer. Protein was quantified and an equal amount of protein was added to each well for SDS-PAGE analysis and subsequent autoradiography and western blotting.

Supplementary Figure Legends

Supplementary Figure S1. Cellular effects of c-Myc and N-Myc activation. (A) Real-time PCR analysis of ornithine decarboxylase (ODC) mRNA levels, a c-Myc target, following treatment of P493-6 cells. Values were normalized to 18s rRNA and expressed as fold-change over control (tet-treated) conditions (n=3 independent experiments, **p-value <0.0008, *p-value <0.05, student's two-tailed t-test), **(B)** P493-6 cells were treated with tetracycline for 24 hours and then washed and cultured for the indicated times, flow cytometric analysis of cell size was quantified by forward scatter with the percentage of 'large' cells expressed as those falling under the gate shown (results are representative of 3 independent experiments), and **(C)** human neuroblastoma SHEP cells expressing N-Myc in a tetracycline-off manner were treated with tetracycline and analyzed for p-eIF2α levels (a tetracycline dose response (upper panel) shows decreased UPR activation with addition of tetracycline, and tetracycline was removed for N-Myc expression to return (lower panel) with a concomitant increase in UPR activation (representative of 2 independent experiments).

Supplementary Figure S2. c-Myc activation and cellular biogenesis and proliferation. (A) ^{35}S labeling was performed in the mycER:PERK$^{fl/fl}$ MEFs, **(B)** nuclear extracts of mycER:PERK$^{fl/fl}$ MEFs confirming activation of myc in the presence of 4-PBA, and **(C)** cell cycle analysis was performed following treatment with 4-HT (50,000 total cells analyzed per sample, value given as ratio of percent G1 over percent S, result is representative of two independent experiments).

Supplementary Figure S3. c-Myc-induced UPR activation. (A) mycER:PERK$^{fl/fl}$ MEFs were infected with an adenovirus expressing Cre recombinase and individual clones were analyzed by RT-PCR to diagnose the absence of PERK transcript, **(B)** RT-PCR and immunoblot analysis of XBP1s in both mycER:PERK$^{fl/fl}$ and mycER:PERK$^{-/-}$ MEFs treated with 4-HT, **(C)** flow cytometric quantitation of cells stained with ER tracker (Figure 2A) (fluorescence was measured from more than 100 cells for each treatment group), and **(D)** P493-6 cells were treated with tetracycline for 24 hours, washed, and flow cytometric analysis of ER-TrackerTM fluorescence was quantified (at least 30,000 viable cells were measured per sample).

Supplementary Figure S4. c-Myc-induced apoptosis in mycER:PERK$^{-/-}$ MEFs. (A) MEFs were treated with 4-HT for 48hrs and cells were examined under phase-contrast microscopy, **(B)** sub-G1 analysis of mycER:PERK$^{fl/fl}$ and mycER:PERK$^{-/-}$ MEFs treated with 4-HT and thapsigargin (values are normalized to controls, *p<0.002, staurosporine (STS) served as a positive inducer of apoptosis), **(C)** infected S51A-eIF2α knock-in MEFs were treated with 4HT and immunoblot analysis was used to detect C-PARP, **(D)** mycER:PERK$^{-/-}$ MEFs were transfected with CMV control or Bcl-xL-expressing

plasmids (WT or ER-targeted cb5), treated with 4-HT, cultured for 72hrs, and stained with crystal violet, **(E-F)** mycER:PERK$^{-/-}$ MEFs were treated with 4-HT (or staurosporine) in the presence of Q-VD-OPH (or negative control peptide) and cytotoxicity was measured by cleaved-PARP (E) and modified clonogenic assay (F) (representative of 2 independent experiments; *p-value <1.9x10^{-13}, student's two-tailed t-test), **(G)** mycER:PERK$^{-/-}$ MEFs were treated with 4-HT for 28h or thapsigargin (500nM for 4h) and intracellular calcium was measured by Fura-2AM fluorescence and microscopy (*p-value <0.0005, student's two-tailed t-test), and **(H)** mycER:PERK$^{-/-}$ MEFs were treated with 4-HT in the presence of the Ca2+ chelator BAPTA-AM (10 μM) and immunoblot analysis was performed to detect cleaved-PARP (representative of more than 3 independent experiments, thapsigargin was used at 10 nM for 1 hour).

Supplementary Figure S5. Cytoprotective autophagy in mycER:PERK$^{flox/flox}$ MEFs and P493-6 cells. (A) MEFs were treated with 500nM thapsigargin and immunoblot analysis was performed to detect the processing of the autophagic marker LC3 (arrow denotes LC3II processed band, blots are representative of 2 independent experiments), **(B)** flux assay measuring LC3 processing in the presence of pepstatin A and E64d, **(C)** P493-6 cells were treated with tetracycline for 24 hours and then washed and cultured for the indicated times; flow cytometric analysis of LysoTracker® mean fluorescence was quantified (results are representative of 2 independent experiments), **(D)** mycER:PERK$^{fl/fl}$ MEFs were treated with bafilomycin A1 (BafA1) and 4-HT and cleaved PARP levels were analyzed, **(E-F)** mycER:PERK$^{fl/fl}$ MEFs were treated with Spautin-1 and 4-HT and LC3II (E) and cleaved PARP (F) levels were detected, **(G)** Atg5+/+ and Atg5-/- MEFs were infected with a retrovirus expressing mycER, treated with 4-HT and analyzed for clonogenic survival (*p<0.0015), and **(I)** PCR analysis of PERK excision in infected PERKfl/fl;CreER bone marrow cells.

Supplementary Figure S6. Myc-dependent UPR-associated gene signature in human Burkitt's lymphoma cells. Meta analysis of array data from Mertz et al. (2). Raji (human Burkitt's lymphoma) cells were treated for eight hours with the BET bromodomain inhibitor JQ1, or inactive enantiomer. A UPR-associated gene signature consisting of DDIT3 (CHOP), c-MYC, XBP1 and ATF3 was uploaded and the data subjected to hierarchical clustering using a Pearson complete correlation coefficient with median centering and log transformation. High (red) and low (green) gene expression is shown for each individual sample.

Supplementary References

1. Li, C., Chen, P., Palladino, A., Narayan, S., Russell, L.K., Sayed, S., Xiong, G., Chen, J., Stokes, D., Butt, Y.M., et al. 2010. Mechanism of hyperinsulinism in short-chain 3-hydroxyacyl-CoA dehydrogenase deficiency involves activation of glutamate dehydrogenase. *J Biol Chem* 285:31806-31818.
2. Mertz, J.A., Conery, A.R., Bryant, B.M., Sandy, P., Balasubramanian, S., Mele, D.A., Bergeron, L., and Sims, R.J. 2011. Targeting MYC dependence in cancer by inhibiting BET bromodomains. *PNAS* 108:16669-16674.
3. Floratos, A., Smith, K., Ji, Z., Watkinson, J., and Califano, A. 2010. geWorkbench: an open source platform for integrative genomics. *Bioinformatics* 26:1779-1780.
4. Harding, H.P., Zhang, Y., Zeng, H., Novoa, I., Lu, P.D., Calfon, M., Sadri, N., Yun, C., Popko, B., Paules, R., et al. 2003. An Integrated Stress Response Regulates Amino Acid Metabolism and Resistance to Oxidative Stress. *Mol Cell* 11:619-633.